

Measuring the Lifetime of Trapped Sleptons Using the General Purpose LHC Detectors

James Pinfold*

Physics Department, University of Alberta, Edmonton, Alberta T6G 2N6

E-mail: pinfold@phys.ualberta.ca

Logan Sibley,

Physics Department, University of Alberta, Edmonton, Alberta T6G 2N6

E-mail: logans@phys.ualberta.ca

ABSTRACT: In supergravity where the gravitino is the lightest supersymmetric particle (LSP), the next-to-lightest supersymmetric particle (NLSP) decays to the gravitino with a naturally long lifetime ($10^4 - 10^8$ s). However, cosmological constraints favour charged sleptons with lifetimes below a year as the natural NLSP candidate. For this scenario we report a method to accurately determine the slepton lifetime and SUSY cross-section from observation of the decays of sleptons trapped in the material comprising the main detector (ATLAS, CMS). A measurement of the lifetime to 5% is possible after 3 years at nominal luminosity and running conditions. This method is sensitive to the cosmologically preferred stau lifetime of ~ 37 days and does not require the use of ancillary trapping volumes.

KEYWORDS: long lived particles, exotic, slepton, supersymmetry, LHC detectors.

*Communicating author

Contents

1. Introduction	1
2. Slepton Properties	3
3. The Model of the Detector and its Surroundings	3
4. The Monte Carlo Simulation	5
5. Triggering on Trapped Slepton Decay	6
6. Backgrounds	7
7. Slepton Lifetime Determination	8
8. Conclusion	11
Appendices	12

1. Introduction

Most studies of supergravity models assume the lightest supersymmetric particle (LSP) is a standard model superpartner, such as a slepton or neutralino. However, there are theoretically plausible scenarios where the gravitino is the LSP [1] [2] [3] [4] [5] [6] [7] [8] [9] [10] [11]. Here the gravitino is a “superWIMP” with a weak scale mass of ~ 100 GeV and couplings suppressed by the reduced Planck scale (RPS), $M_{RPS} = \sqrt{8\pi G_N}$, where G_N is the gravitational constant. If the gravitino is the LSP, the next-to-lightest supersymmetric particle (NLSP) decays to its standard model partner and a gravitino. The NLSP is a weak-scale particle decaying gravitationally and so has a natural lifetime of the order of: $M_{RPS}^2/M_{weak}^3 \sim 10^4$ - 10^8 s (τ_{NLSP}). This extraordinarily long lifetime renders the decay of the NLSP particle undetectable in a typical collider detector.

The superWIMP is a good candidate for dark matter and as such the gravitino LSP scenario is constrained by measurements of non-baryonic cold dark matter density. The NLSP decays will deposit electromagnetic [12] and hadronic [13] energy into the universe, which may upset the successful predictions of standard big bang nucleosynthesis (BBN). Also, it is possible these NLSP decays may distort the cosmic microwave background (CMB) from its observed Planckian spectrum. In addition, photons produced in NLSP decays are subject to bounds on the diffuse photon flux. However, it turns out the superWIMP scenario can satisfy all these constraints.

Neutralino NLSPs are highly disfavored [7] [11]. However, slepton and sneutrino NLSP scenarios have been analyzed and found to be safe [6][7] with the result that the most natural NLSP candidates are sleptons, particularly the right-handed stau. Cosmological constraints exclude the upper range of τ_{NLSP} since, if the decays occur in a colder universe, then the decay products would not be effectively thermalized. The CMB and BBN constraints, for typical thermal relic NLSP abundances, provide an upper bound on NLSP lifetimes that excludes τ_{NLSP} above roughly a year.

Late NLSP decays may even resolve the leading BBN ${}^7\text{Li}$ anomaly by reducing the predicted ${}^7\text{Li}$ abundance to the low values favoured by observations [1] [2]. The NLSP lifetime that best resolves the ${}^7\text{Li}$ anomaly is 3×10^6 s [4], of the order of a month. Another motivation follows from considerations of leptogenesis [14]. In the gravitino LSP scenario, the gravitino does not decay. Thus, the reheat temperature is bounded only by the overclosure constraint on the gravitino density. For a gravitino mass $M_{\tilde{G}} \sim 100$ GeV, reheat temperatures as high as $\sim 10^{10}$ GeV are allowed consistent with thermal leptogenesis [15][16]. Further connections between gravitino LSPs and leptogenesis are discussed in Ref. [17].

The collider implications of a gravitino LSP with a charged slepton NLSP with lifetime under (but not much under) a year have been investigated [19]. In particular, the possibility of trapping sleptons in material (water tanks) placed just outside Large Hadron Collider (LHC) or International Linear Collider (ILC) detectors was investigated. In this approach the material in which the sleptons are trapped is moved to an underground location (underground reservoirs) in order that slepton decays may be observed in a relatively background-reduced environment. At the Large Hadron Collider (LHC), the investigators found that, depending on the mass scale of supersymmetry and the luminosity of the machine, tens to thousands of sleptons may be trapped each year. This implies that percent level studies of sleptons may be performed with resulting insights into supergravity, supersymmetry breaking, dark matter and dark energy [19].

In this paper, we report a method of measuring the slepton lifetime in a typical LHC detector modelled on ATLAS, using the decays of sleptons trapped in the detector itself. No use is made of additional water traps or underground reservoirs. The cosmic ray background is essentially eliminated by the depth of the detector underground (~ 100 m) and by only utilizing upward going slepton decays. The background from upward going neutrino interactions, giving rise to upward going muons, is eliminated by considering only upward going decay products originating from inside a fiducial volume defined to be within the outer RPC and TGC layers.

Our analysis shows that definite evidence of the existence of the decays of trapped sleptons would be available in the first year of running with a received luminosity of 10 fb^{-1} . A measurement of the lifetime to 4% is possible after 3 years at nominal luminosity and running conditions and a received luminosity of 120 fb^{-1} . An observation of a trapped slepton signal in this manner would presumably justify the more extensive and expensive water traps and instrumented reservoirs discussed elsewhere.

2. Slepton Properties

Current collider bounds from the null searches for long lived tracks at LEP-II [20] require the slepton mass ($m_{\tilde{l}}$) to be greater than 99 GeV. Cosmology also has something to say about the slepton mass. In the gravitino superWIMP dark matter scenario, assuming that superWIMPS provide most, if not all, of the cold non-baryonic dark matter with density in the range $0.094 < \Omega_{DM} h^2 < 0.124$, the mass of the slepton is constrained to the range $m_{\tilde{l}} \sim 700\text{-}1000$ GeV. Sleptons this heavy will be difficult to study at the LHC.

However, if gravitinos are produced during reheating, then for the reheating temperatures preferred for leptogenesis as discussed above ($\sim 10^9$ GeV), gravitinos could form all of the non-baryonic dark matter for slepton masses as low as 120 GeV [21]. Alternatively, if the neutralino ($\tilde{\chi}$) is slightly heavier than the slepton, then it will freeze out at the same time as the slepton and then decay to the slepton, thus combining its relic density with that of the slepton. This permits much lower slepton masses to produce the correct gravitino dark matter density. For example, in minimal supergravity (mSUGRA) with $A_0 = 0$, $\tan\beta = 10$, and $\mu > 0$, the required relic density may be achieved in the region $\tilde{\tau}_{LSP} \tilde{\chi}_{LSP}$ at $M_{1/2} = 300$ GeV, where $M_{\tilde{\tau}} \approx M_{\tilde{\chi}} \approx 120$ GeV [22]. When the gravitino is not the LSP, this is in the excluded stau LSP region.

Assuming the lepton mass is negligible, the width of the slepton decay $\tilde{l} \rightarrow l\tilde{G}$ is:

$$\Gamma(\tilde{l} \rightarrow l\tilde{G}) \rightarrow \frac{1}{48\pi M_{RPS}^2} \frac{M_{\tilde{l}}^5}{M_{\tilde{G}}^2} \left[1 - \frac{M_{\tilde{G}}^2}{M_{\tilde{l}}^2} \right]^4 \quad (2.1)$$

As the gravitino decays gravitationally, the decay is determined only by the lepton mass, the gravitino mass and the Planck mass - no SUSY parameters enter.

In the scenario considered in this paper where the gravitino is the LSP, the lower bound on $M_{1/2}$ (300 GeV) is determined by the requirement of a stau NLSP. The number of trapped staus generated rapidly diminishes as $M_{1/2}$ increases and an upper bound on $M_{1/2}$ ($= 800$ GeV/ c^2) can be defined to be where only a few staus may be trapped in ATLAS per year.

Knowledge of the slepton range in matter is a key aspect of this analysis. Charged particles passing through matter lose energy by emitting radiation and by ionizing atoms. In this analysis, we assume the slepton loses energy in a similar way to a very heavy muon of the same mass, where ionization losses dominate over energy loss by radiation. In this case, the GEANT3 simulation package [18] was used to estimate the range. Another author [19] directly estimated the energy loss of the slepton per gcm^{-2} using the Bethe Bloch formula. The results of the GEANT simulation are in excellent agreement with the direct calculation for the range of a stau.

3. The Model of the Detector and its Surroundings

The ATLAS detector and experiment caverns, and the ATLAS rock overburden and underburden are all modelled in GEANT 3.21 [18]. Our detector model, shown in Figure 2, is

based closely on the ATLAS detector [23], as described in the ATLAS Technical Design Reports [24]. This model includes the beam pipe and shielding, the inner detector (the pixel detector, the semiconductor tracker (SCT) and the transition radiation tracker (TRT)), the calorimetry (the electromagnetic calorimeter (ECAL), the hadronic tile calorimeter (HCAL), the liquid argon endcap calorimeter (LAr) and the forward calorimeter (FCAL)), the magnet system (the barrel solenoid and the barrel and endcap toroids) and the muon system (the monitored drift tube chambers (MDT), the cathode strip chambers (CSC), the resistive plate chambers (RPC) and the thin gap chambers (TGC)).

All volumes are filled with a material that is a smeared average of the materials found in the corresponding actual detector volumes, where these averages correspond to the radiation lengths of each of the ATLAS components. An ideal toroidal field is used to model the magnetic field inside the barrel and endcap toroid models, and the barrel solenoid has a uniform field of 2 T.

The muon system, particularly the RPCs and TGCs, has the most direct impact on this study of trapped stau decay. The RPCs and TGCs are dedicated trigger layers and, in combination with the precision of the MDTs, can allow the muon system to stand on its own as a muon detector. The RPCs lie in the barrel section of the detector and are separated into three layers. The central layer is referred to as the pivot layer, where hits in this layer are projected outward to the inner and outer RPC layers in coincidence windows (cones about the direction of the incoming muon that are dependent on the muon's transverse ¹ momentum) to search for matching hits. The outer layer is used only to search for high transverse momentum muons. The TGCs are split into five layers in each of the ATLAS endcap sections. All but one of these layers is in the form of a doublet, containing two

¹The transverse direction is orthogonal to the direction of the beam.

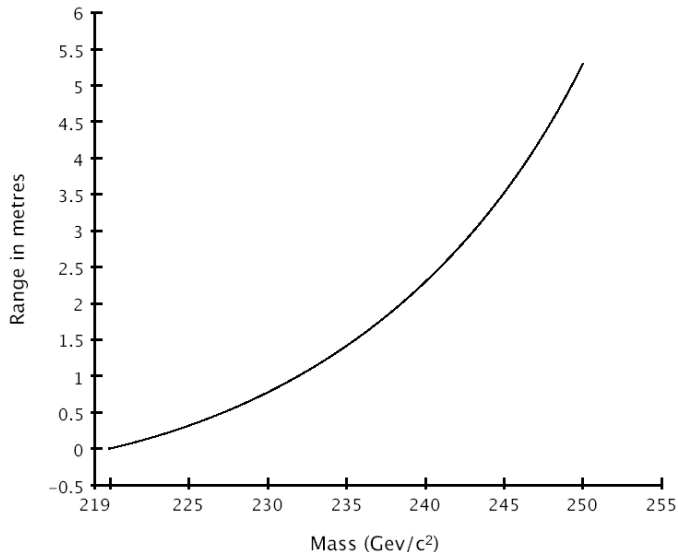


Figure 1: The range in lead of a stau with mass 219 GeV c^{-2} as a function of energy, estimated using a GEANT3 simulation of the stau range.

carbon dioxide- n -pentane gas volumes that are each layered between graphite cathodes and separated by paper honeycomb. The other TGC layer is a triplet, consisting of three gas volumes. The outermost doublets are the endcap pivot layers, where hits there are projected inward to the other TGC layers and matching hits are searched for in the same fashion as the RPCs.

4. The Monte Carlo Simulation

An R-parity conserving mSUGRA SUSY breaking model is assumed, with the common scalar mass m_o and the common soft breaking parameter A_o taken to be 0 GeVc, the ratio of the Higgs vacuum expectation values $\tan\beta$ is taken to be 10, the sign of the higgsino mass term μ taken to be greater than 0, and the common gaugino mass $M_{1/2}$ varied between 300 GeV and 800 GeV in increments of 100 GeV. This one-dimensional parameter set lies in a region of the mSUGRA parameter space that requires the gravitino to be the LSP, otherwise it would be an excluded stau LSP region [19]. The lower bound on $M_{1/2}$ was chosen to have a stau NLSP, and the upper bound is chosen so that the SUSY cross-section is high enough to have enough staus created each year to make this analysis useful. Table 1 lists the SUSY cross-section that corresponds to each value $M_{1/2}$.

$M_{1/2}$ (GeV)	300	400	500	600	700	800
σ_{SUSY} (pb)	20.2	4.87	1.51	0.542	0.219	0.096

Table 1: The SUSY cross-sections that correspond to the values of $M_{1/2}$ considered.

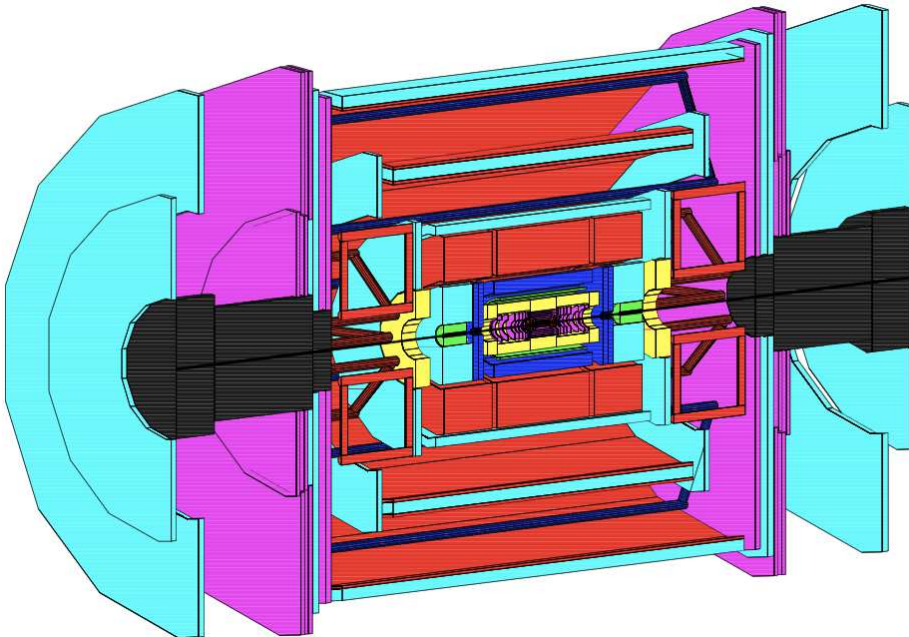


Figure 2: GEANT model of an LHC detector based closely on ATLAS.

To study trapped stau decay, the proton-proton collisions of the LHC are simulated using HERWIG 6.507 [25] interfaced with ISAJET 7.71 [26] in order to obtain the SUSY mass spectrum. We consider sparton, gaugino and/or slepton production generated using IPROC=3000 [27] where the three following processes are implemented:

- 2-parton \rightarrow 2-sparton processes. All QCD sparton, i.e. squark and gluino, pair production processes are implemented;
- 2-parton \rightarrow 2-gaugino or gaugino+sparton processes. All gaugino, i.e. chargino and neutralino, pair production processes and gaugino-sparton associated production processes are implemented; and,
- 2-parton \rightarrow 2-slepton processes. All Drell-Yan slepton production processes are implemented.

The stau lifetimes that we consider are 7, 30 and 90 days. Each stau is given a random creation time throughout a year during those periods when the LHC beam is on, and a random decay time according to its lifetime spectrum.

After being assigned a lifetime, creation time and decay time, the staus are passed through the GEANT ATLAS model. GEANT tracks the staus until the stau momentum falls below $0.001 \text{ GeV}/c^2$, at which point it is assumed the stau has become trapped. It is also assumed that all staus will stop before decaying ². Also, because the stau is heavy and has an electromagnetic but not a colour charge, GEANT treats it like an extremely massive muon as it travels through matter, losing most of its energy through ionization effects.

Once the stau has stopped in ATLAS, it is decayed by GEANT, and the resulting muons and pions down the decay chain are tracked as they pass through ATLAS. At that point, a model trigger decision is applied that mimics the decision made by the cosmic ray muon trigger. Based on [28], it is assumed that the trigger in the barrel region has an 83% efficiency, and the trigger in the endcap region has a 95% efficiency.

5. Triggering on Trapped Slepton Decay

Once the LHC attains its design luminosity of $10^{34} \text{ cm}^{-2}\text{s}^{-1}$, ATLAS will become subject to more than 10^9 events per second. Because of their high cross-sections, QCD processes will dominate these events and any rare signals, like SUSY processes, will be swamped by this background. However, ATLAS utilizes a three-tier trigger system to extract these rare events and successively reduce the data rate to a final recordable rate of approximately 200 Hz.

The low-level trigger, level 1 (LVL1), is hardware-based and consists of custom electronics operating at the LHC bunch crossing frequency of 40 MHz with a latency time of just $2.5 \mu\text{s}$. Up to 256 distinct trigger types that rely on information from the calorimeters

²This is valid because the lifetimes considered here are much greater than the time required for the stau to travel even 1 km away from ATLAS through the rock overburden or underburden.

and muon detectors may be programmed into the LVL1 trigger menus. The level 2 (LVL2) trigger and event filter (EF) make up the software-based high-level trigger that runs on dedicated processor farms.

The ATLAS cosmic ray trigger consists of a set of dedicated LVL2 cosmic ray muon trigger algorithms that rely heavily on the LVL1 muon trigger architecture. In the barrel region, the LVL1 cosmic ray muon trigger [29] requires coincidences in both the η and ϕ directions of the inner two RPC layers. If the RPC pivot layer registers a hit, then the trigger searches for a coincidence in the inner RPC layer across all sectors of the inner RPC layer that are electrically connected. This loosens the pointing requirement that is inherently built into most LVL2 trigger algorithms, and corresponds approximately to the muon pointing to within 2 m of the interaction point. The timing of the cosmic rays is determined using the MDT chambers.

The physical cross-section of the TGC endcaps is very small with respect to the cosmic ray muons that arrive from above essentially parallel to the TGC surface. Consequently, to boost the number of triggers that can occur, dummy hits are introduced into the large wheels to force a trigger to fire when only a single layer of the TGC triplet is actually hit. Since the layers of the TGC triplet are so closely spaced, any particle originating from the interaction point will likely register a hit in all three layers, with a track that may be traced back to the interaction point and that has a matching track in the inner detector. Cosmic ray muons will generally not point to the interaction point, so they are easily distinguished as cosmic rays.

According to ATLAS, then, the signal of the trapped staus will look very similar to that of cosmic ray muons. The stau decay products will not generally originate from the interaction point, nor will they fit nicely into the bunch crossing periods of the LHC. As such, the ATLAS cosmic ray muon trigger is a natural choice to search for the signal of the trapped stau decay. Because the cosmic ray trigger can perform precision timing of the muons, it will also work for decay products originating both from within and outside of ATLAS for staus trapped either within ATLAS or in the rock surrounding the main ATLAS experiment cavern.

6. Backgrounds

In order to eliminate the overwhelming background produced by the proton-proton collisions, as well as the background from beam-halo and beam-gas rates [30], we propose to search for the signal of trapped stau decay only when the LHC beam is off. The only remaining background sources to the trapped stau signal arise from cosmic rays and upward-going neutrino-induced muons. Neutrino-induced upward-going staus may also be a possibility [31].

ATLAS is bombarded by cosmic ray muons at a rate of kHz, which would likely completely shadow the trapped stau signal. This large flux can be immediately dealt with by discarding all downward-going tracks, which is well within the capacity of the ATLAS trigger. While this would cut the number of signal events roughly in half, the signal to background ratio will be significantly enhanced by only considering upward-going events.

$M_{1/2}$ (GeV)	7 days			30 days			90 days		
300	713.6	\pm	14.5	709.5	\pm	34.8	693.8	\pm	21.5
400	673.1	\pm	72.4	705.1	\pm	23.0	718.9	\pm	20.3
500	722.8	\pm	29.0	706.3	\pm	27.1	702.2	\pm	15.2
600	713.8	\pm	37.1	702.5	\pm	27.8	685.5	\pm	19.9
700	703.5	\pm	32.0	708.8	\pm	29.2	716.4	\pm	8.2
800	706.3	\pm	33.7	702.6	\pm	20.3	693.0	\pm	13.5

Table 2: Acceptance ($\times 10^6$) of the ATLAS-like detector, defined as the total number of upward-going stau decay products observed by the model trigger relative to the total number of Monte-Carlo staus produced, from staus that are trapped within the fiducial volume.

The background from upward-going muons created in interactions in the rock beneath ATLAS can also be eliminated. The “ATLAS-like” cosmic ray trigger considered here requires that the particle must pass through the inner two RPC layers and within 2m of the interaction point (in the barrel region), or it must pass through the innermost TGC layer (in the endcap). In order to rule out muons entering ATLAS from below, we restrict the trapping region for the staus comprising our signal to be inside the outer RPC layer (within a radius of 1027.5 cm) and inside the inner TGC layer (inside a z half-length of 1291 cm). We also require the particles to be upward going. Looking only at particles trapped within the above-defined fiducial volume, we can be sure that we are not seeing anything but signal.

7. Slepton Lifetime Determination

The ratio of the number of stau decays seen by the model trigger to the total number of staus created gives the geometric detector acceptance, α . Table 2 gives α for upward-going staus trapped within the fiducial volume as a function of both $M_{1/2}$ and lifetime, where a total of 10^6 staus were produced at each point and α is an average over six different trials.

The number of candidate stau decays that ATLAS will be sensitive to during a period when the beam is off will be proportional to the geometric acceptance α multiplied by the stau production rate. Thus, the number of candidate stau decays ATLAS will detect during a shutdown period as a function of elapsed time will be:

$$N_{hits} = \alpha N_{8,j}^f e^{-t/\tau}, \quad (7.1)$$

where τ is the stau lifetime, t is the amount of time since the beam shut off and $N_{8,j}^f$ is the number of trapped staus at beam shut off (see the Appendix for the complete definition). To increase the size of the data set, a sum over multiple years can be taken, leading to

$$N_{hits} = \alpha \left(\sum_{j=1}^n N_{8,j}^f e^{-t/\tau} \right), \quad (7.2)$$

where n is the number of years considered.

This proportionality may be expressed as

$$N = Ae^{-Bt} \quad (7.3)$$

$$A = \alpha \sum_{j=1}^n N_{8,j}^f \quad (7.4)$$

$$B = \frac{1}{\tau}. \quad (7.5)$$

As such, it is possible to model-independently determine the lifetime of the stau using equation 7.3 to fit the distribution of the total number of candidate stau decay products seen as a function of elapsed time during a beam shut off period. The SUSY cross-section is embedded in the value of A (see equation 7.4), and may thus be determined, although the dependence of A on α makes this model-dependent.

Two scenarios are considered in this analysis. The first assumes the LHC has run for only one year at low luminosity (an integrated luminosity of 10 fb^{-1}). The second scenario assumes that three years worth of data have been collected, with two years of LHC running at low luminosity (as above) and one year of LHC running at high luminosity (an integrated luminosity of 100 fb^{-1}). An analysis completed after only one year of LHC running could be used to demonstrate whether a decay signal may be seen. Combining three years worth of data would allow for a more accurate determination of the lifetime of the decaying particle, while still within a reasonable amount of time to see results.

The LHC operating schedule is taken from [35] [36], which results in 200 days of beam running, segmented by 3 day beam shut off periods and a large 144 day beam shut down period over the winter. We use this large shut down period³, where the assumed lifetimes of 7, 30 and 90 days are shorter than the total amount of time the beam is off.

To determine the statistical spread in these values, this fit was performed on 400 distinct data sets for each scenario, using lifetimes of 7, 30 and 90 days, over the entire range of $M_{1/2}$. We only attempted this fit when the expected number of events was greater than ten with the bin size set so that there were at least 4 events in the first bin. Figure 3 shows, as an example, a distribution of the number of stau decays versus the elapsed time during the shutdown period, summing over 3 years of data (2 years at low luminosity and 1 year at high luminosity). The solid curve depicts the fit to the data that gives the stau lifetime as 29.9 ± 1.5 days (model independent) and the SUSY cross-section as 18.9 ± 1.3 pb. Figure 4 shows the distribution of lifetimes obtained for 400 experiments, under the second scenario, for a true stau lifetime of 30 days at $M_{1/2} = 300 \text{ GeV}/c^2$. In Figure 5, we see the corresponding distribution of number of events for the 400 experiments, and in Figure 6 the distribution of the SUSY cross-section values.

Tables 3, 4 and 5 give the results for the both scenarios where the slepton lifetimes are 7 days, 30 days and 90 days, respectively. One can see for all scenarios that, as the value of $M_{1/2}$ increases, the SUSY cross-section decreases and, consequently, so does the accuracy of the stau lifetime and SUSY cross-section determination using trapped staus.

³If the lifetime of the stau is not long compared to the 3 day shut off periods, then those periods could be used to perform this analysis, as well. This possibility is not considered here.

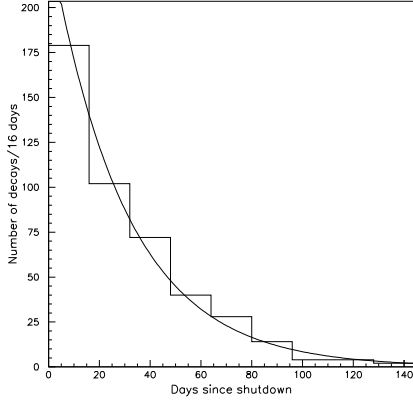


Figure 3: Sum over 3 years of data (2 years low luminosity and 1 year high luminosity) of the number of stau decay products seen by the model trigger as a function of elapsed time during the shutdown period. The fit of the distribution results in a lifetime of 29.9 ± 1.5 days and a SUSY cross-section of 18.9 ± 1.3 pb.

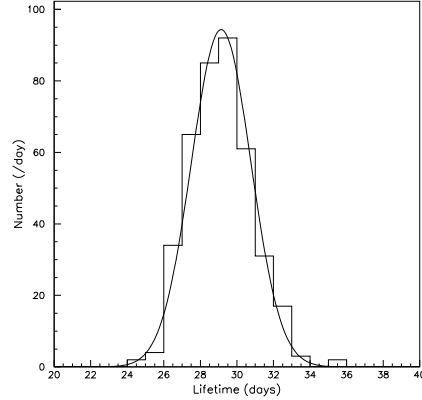


Figure 4: The lifetime distribution for 400 experiments under the second scenario where the true stau lifetime is 30 days and the value of $M_{1/2}$ is $300 \text{ GeV}/c^2$.

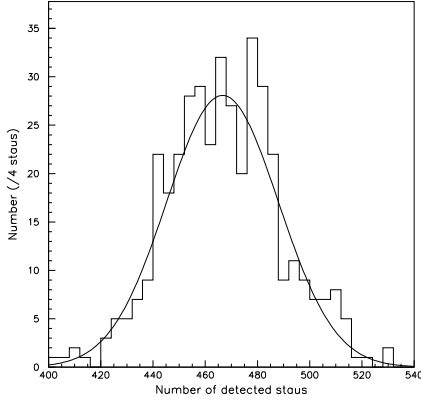


Figure 5: The distribution of the number of events for 400 experiments under the second scenario where the true stau lifetime is 30 days and the value of $M_{1/2}$ is $300 \text{ GeV}/c^2$.

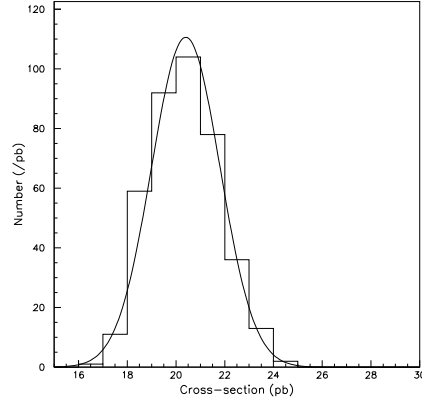


Figure 6: The SUSY cross-section distribution for 400 experiments under the second scenario where the true stau lifetime is 30 days and the value of $M_{1/2}$ is $300 \text{ GeV}/c^2$.

For $\tau = 30$ days, near the cosmologically preferred value of the stau lifetime (37 days), our results show (see Table 4) that under Scenario 1 for $M_{1/2} \sim 300\text{-}400 \text{ GeV}$ and SUSY cross-section $\sigma_{SUSY}=20.2\text{-}4.87 \text{ pb}$ the stau lifetime and σ_{SUSY} determined agree with the actual values within a fractional (statistical) error on the measured value of $\sim \pm(25\%\text{-}60\%)$. Under this scenario we obtain $\sim 40\text{-}10$ signal events after 1 year running at low luminosity. For scenario 2, for $M_{1/2} \sim 300\text{-}600 \text{ GeV}$ with $\sigma_{SUSY}=20.2\text{-}0.54 \text{ pb}$ we can obtain a lifetime

and cross-section estimate that agrees with the set values within a fractional statistical uncertainty on the measured value of $\sim \pm(5\%-60\%)$ and $\sim \pm(7\%-70\%)$, respectively, with ~ 467 -13 signal events detected.

Under Scenario 1, for a relatively short stau lifetimes of 7 days, we only have sensitivity for $M_{1/2} \sim 300$ GeV with cross-section $\sigma_{SUSY}=20.2$ pb. In this case, the stau lifetime and SUSY cross-section determined agrees with the actual value to within the fractional (statistical) uncertainty of $\sim \pm 50\%$ and $\sim \pm 80\%$, respectively, on the measured value, with ~ 10 signal events detected. We can do better under scenario 2 where, for $M_{1/2} \sim 300$ -500 GeV and $\sigma_{SUSY} = 20.2$ -1.51 pb, we can determine the stau lifetime and σ_{SUSY} to within the fractional (statistical) uncertainty on the measured value of $\sim \pm(12\%-65\%)$. In this case the number of detected events varies between ~ 120 and ~ 10 .

The longest stau lifetime considered is 90 days. For Scenario 1 we have sensitivity for $M_{1/2} \sim 300$ -400 GeV/ c^2 and $\sigma_{SUSY} = 20.2$ -4.87 pb. Under this scenario, we can determine the stau lifetime σ_{SUSY} to within the fractional (statistical) uncertainty on the measured value of $\sim \pm(23\%-30\%)$ and $\sim \pm(13\%-24\%)$, respectively, with the number of recorded signal events varying between ~ 83 and ~ 21 . For scenario 2, we can measure the stau lifetime over the range $M_{1/2} \sim 300$ -700 GeV/ c^2 and $\sigma_{SUSY} = 20.2$ -0.22 pb. In this case, we can pin down the stau lifetime and σ_{SUSY} to within the fractional (statistical) uncertainty on the measured value of $\sim \pm(7\%-40\%)$ and $\sim \pm(4\%-48\%)$, respectively, with the number of detected events varying between ~ 990 and ~ 12 .

8. Conclusion

The sensitivity of the ATLAS-like detector to the decay of long-lived staus that become trapped in the detector was studied using a simplified model of the ATLAS detector. To completely eliminate the background from cosmic rays and upward going neutrino-induced muons, only upward-going decay products originating from inside a fiducial volume defined to be within the outer RPC and TGC layers were studied. In addition, decays were only recorded during beam-off periods to further reduce backgrounds from actual collisions.

By fitting the number of candidate stau decay products detected by a model cosmic ray muon trigger during periods when the LHC beam is off as a function of the elapsed time during the beam shut off period, the model-independent stau lifetime and the model-dependent SUSY cross-section can be determined.

The fitting procedure returns the stau lifetime and SUSY cross-section with up to approximately 5% statistical accuracy on the measured value. For almost all situations considered that allow a fit - those with ~ 10 detected events or more - the measured values of the slepton lifetime and SUSY cross-section lie within $\pm 1\sigma$ of the actual value, where σ is the statistical error on the measured value. We found that for the two running scenarios considered, our analysis procedure has a good sensitivity to slepton lifetimes of ~ 30 days and a SUSY cross-section greater than approximately 0.50 pb. It is interesting to note that stau lifetimes (~ 30 days) are cosmologically favoured by models propounding a gravitino LSP scenario.

$M_{1/2}$ (GeV)	Scenario	1 year low	2 years low	1 high	Expected
300	τ	6.8 \pm 3.5	6.8 \pm 0.8		7
	σ_{SUSY}	9.5 \pm 7.3	20.9 \pm 3.2		20.2
	N_{hits}	10.2 \pm 2.8	120.8 \pm 10.5		10.0/119.9
400	τ	—	7.3 \pm 2.7		7
	σ_{SUSY}	—	4.52 \pm 1.75		4.87
	N_{hits}	2.4 \pm 1.6	27.7 \pm 4.5		2.3/27.3
500	τ	—	9.62 \pm 6.31		7
	σ_{SUSY}	—	0.73 \pm 0.48		1.51
	N_{hits}	—	9.7 \pm 2.8		0.8/9.1
600	τ	—	—		7
	σ_{SUSY}	—	—		0.54
	N_{hits}	—	3.4 \pm 1.8		0.3/3.2
700	τ	—	—		7
	σ_{SUSY}	—	—		0.22
	N_{hits}	—	1.3 \pm 1.6		0.1/1.3
800	τ	—	—		7
	σ_{SUSY}	—	—		0.096
	N_{hits}	—	—		0.1/0.6

Table 3: Fitted and expected values of stau lifetime, SUSY cross-section and number of events for a stau lifetime of 7 days at both luminosity scenarios. The unit of lifetime is days and that of cross-section is picobarns.

Appendices

If we set the luminosity for year j of running at the LHC to be L_j , then the stau production rate at ATLAS, assuming R-parity conservation, will be

$$R_j = 2 \frac{L_j \sigma_{SUSY}}{T_{on}}, \quad (1)$$

where T_{on} is the total time over a year that the beam is on. The schedule of beam operation assumed is given in [35][36], which gives a total of 200 days of LHC beam operation in one year. The integrated luminosity of the LHC is assumed to be 10 fb^{-1} and 100 fb^{-1} for low and high luminosity years, respectively.

Now, letting the number of undecayed staus remaining in or around ATLAS at beam turn-on be N^o and the number remaining at beam turn-off be N^f , the number of staus remaining as a function of time t becomes

$$\begin{aligned} N_{off} &= N^f e^{-t/\tau} \\ N_{on} &= N^o e^{-t/\tau} + R\tau(1 - e^{-t/\tau}), \end{aligned} \quad (2)$$

where τ is the stau lifetime.

$M_{1/2}$ (GeV)	Scenario	1 year low	2 years low	1 high	Expected
300	τ	29.3 \pm 7.3	29.1 \pm 1.6		30
	σ_{SUSY}	19.9 \pm 5.1	20.4 \pm 1.4		20.2
	N_{hits}	39.7 \pm 6.2	466.6 \pm 21.5		39.7/476.6
400	τ	33.9 \pm 19.9	29.1 \pm 3.6		30
	σ_{SUSY}	2.83 \pm 1.71	4.97 \pm 0.72		4.87
	N_{hits}	10.1 \pm 2.8	112.6 \pm 10.4		9.5/114.2
500	τ	—	31.6 \pm 8.1		30
	σ_{SUSY}	—	1.37 \pm 0.54		1.51
	N_{hits}	2.9 \pm 2.1	34.8 \pm 5.7		3.0/35.5
600	τ	—	35.2 \pm 21.2		30
	σ_{SUSY}	—	0.36 \pm 0.26		0.54
	N_{hits}	—	13.0 \pm 3.5		1.1/12.6
700	τ	—	—		30
	σ_{SUSY}	—	—		0.22
	N_{hits}	—	5.6 \pm 2.1		0.4/5.2
800	τ	—	—		30
	σ_{SUSY}	—	—		0.096
	N_{hits}	—	2.8 \pm 2.3		0.2/2.2

Table 4: Fitted and expected values of stau lifetime, SUSY cross-section and number of events for a stau lifetime of 30 days at both luminosity scenarios. The unit of lifetime is days and that of cross-section is picobarns

Using equation 2 and labelling the eight LHC operating periods with the index i gives

$$\begin{aligned}
N_{1,1}^o &= 0 \\
N_{1,j}^o &= N_{8,j-1}^f e^{-t_{sd}/\tau}, j \geq 2 \\
N_{i,j}^o &= N_{i-1,j}^f e^{-t_{off}/\tau}, i \in [2, 8] \\
N_{i,j}^f &= N_{i,j}^o e^{-t_{on}/\tau} + R_j \tau (1 - e^{-t_{on}/\tau}),
\end{aligned} \tag{3}$$

where t_{sd} , t_{off} and t_{on} are the amounts of time during a shutdown, offline and operational period of the LHC ⁴. This set of equations can be used to determine the number of undecayed staus remaining at the beginning and end of each operational period, resulting in

$$\begin{aligned}
N_{i,j}^f &= N_{1,j}^o e^{-i(t_{off}+t_{on})/\tau} e^{t_{off}/\tau} + \\
&\quad R_j \tau (1 - e^{-t_{on}/\tau}) \sum_{n=0}^{i-1} e^{-n(t_{off}+t_{on})/\tau} \\
N_{1,j}^o &= \sum_{m=1}^{j-1} R_m \tau (1 - e^{-t_{on}/\tau}) \sum_{n=0}^7 e^{-n(t_{off}+t_{on})/\tau}.
\end{aligned}$$

⁴The shutdown period is a long 144 day period when the beam is shut off and the offline periods are short three day down times between beam operational periods.

$M_{1/2}$ (GeV)	Scenario	1 year low		2 years low 1 high		Expected
300	τ	87.5	± 20.4	89.0	± 6.0	90
	σ_{SUSY}	20.2	± 2.6	19.9	± 0.8	20.2
	N_{hits}	82.8	± 9.1	989.9	± 30.9	83.7/1007.9
400	τ	65.4	± 19.7	87.6	± 10.7	90
	σ_{SUSY}	5.06	± 1.20	4.82	± 0.40	4.87
	N_{hits}	20.8	± 4.4	247.9	± 16.3	20.9/251.8
500	τ	—		83.8	± 18.9	90
	σ_{SUSY}	—		1.53	± 0.23	1.51
	N_{hits}	6.7	± 2.6	75.3	± 8.2	6.3/76.3
600	τ	—		66.3	± 18.2	90
	σ_{SUSY}	—		0.59	± 0.13	0.54
	N_{hits}	2.4	± 1.5	26.6	± 5.3	2.2/26.6
700	τ	—		68.8	± 27.8	90
	σ_{SUSY}	—		0.23	± 0.11	0.22
	N_{hits}	—		11.5	± 3.3	0.9/11.3
800	τ	—		—		90
	σ_{SUSY}	—		—		0.096
	N_{hits}	—		5.4	± 3.4	0.4/4.8

Table 5: Fitted and expected values of stau lifetime, SUSY cross-section and number of events for a stau lifetime of 90 days at both luminosity scenarios. The unit of lifetime is days and that of cross-section is picobarns.

$$e^{-(j-1-m)(7t_{off}+8t_{on})/\tau} e^{-(j-m)t_{sd}/\tau}. \quad (4)$$

Meanwhile, the number of staus that decay during shutdown period i of year j is

$$\begin{aligned} N_{i,j}^{decays} &= N_{i,j}^f (1 - e^{-t_{off}/\tau}), \quad i \in [1, 7] \\ N_{8,j}^{decays} &= N_{8,j}^f (1 - e^{-t_{sd}/\tau}). \end{aligned} \quad (5)$$

Thus, the number of decays ATLAS will see will be the the total number of decays that occur during a period when the beam is off multiplied by the geometric detector acceptance α .

References

- [1] J. L. Feng, A. Rajaraman and F. Takayama, Phys. Rev. Lett. **91**, 011302 (2003).
- [2] J. L. Feng, A. Rajaraman and F. Takayama, Phys. Rev. D **68**, 063504 (2003).
- [3] J. L. Feng, A. Rajaraman and F. Takayama, Phys. Rev. D **68**, 085018 (2003).
- [4] J. R. Ellis, K. A. Olive, Y. Santoso and V. C. Spanos, Phys. Lett. B **588**, 7 (2004).
- [5] W. Buchmuller, K. Hamaguchi, M. Ratz and T. Yanagida, Phys. Lett. B **588**, 90 (2004).
- [6] J. L. Feng, S. Su and F. Takayama, hep-ph/0404198.

- [7] J. L. Feng, S. Su and F. Takayama, hep-ph/0404231.
- [8] J. L. Feng, A. Rajaraman and F. Takayama, hep-th/0405248.
- [9] J. R. Ellis, K. A. Olive, Y. Santoso and V. C. Spanos, hep-ph/0408118.
- [10] J. R. Ellis, K. A. Olive, Y. Santoso and V. C. Spanos, hep-ph/0408118.
- [11] L. Roszkowski and R. R. de Austri, hep-ph/0408227.
- [12] M. Kawasaki and T. Moroi, *Astrophys. J.* **452**, 506 (1995); E. Holtmann, M. Kawasaki, K. Kohri and T. Moroi, *Phys. Rev. D* **60**, 023506 (1999); M. Kawasaki, K. Kohri and T. Moroi, *Phys. Rev. D* **63**, 103502 (2001); R. H. Cyburt, J. R. Ellis, B. D. Fields and K. A. Olive, *Phys. Rev. D* **67**, 103521 (2003).
- [13] K. Jedamzik, *Phys. Rev. D* **70**, 063524 (2004); M. Kawasaki, K. Kohri and T. Moroi, astro-ph/0402490; astro-ph/0408426.
- [14] M. Fukugita and T. Yanagida, *Phys. Lett. B* **174**, 45 (1986).
- [15] T. Moroi, H. Murayama and M. Yamaguchi, *Phys. Lett. B* **303**, 289 (1993).
- [16] M. Bolz, A. Brandenburg and W. Buchmuller, *Nucl. Phys. B* **606**, 518 (2001).
- [17] R. Allahverdi and M. Drees, *Phys. Rev. D* **70**, 123522 (2004).
- [18] The GEANT Collaboration, “GEANT Detector Description and Simulation Tool”, CERN Program Library Long Writeup W5013, 1994.
- [19] J. Feng, and B. Smith, *Phys. Rev. D* **71**, 015004 (2005).
- [20] F. Cerutti, M. Fanti, P. Giacomelli, P. Kluit, R. McNeil, C. Rembser and U. Schwickerath, LEPSUSYWG/02-05.1, (2005).
- [21] L. Roszkowski and R. R. de Austri, hep-ph/0408227.
- [22] G. Belanger, F. Boudjema, A. Cottrant, A. Pukhov and A. Semenov, hep-ph/0407218.
- [23] G. Aad *et al.*, “The ATLAS Experiment at the CERN Large Hadron Collider”. *JINST* **3**: S08003, (2008).
- [24] The ATLAS Collaboration, “ATLAS Technical Proposal for a General-Purpose pp Experiment at the Large Hadron Collider at CERN”, CERN/LHCC/94-43, (1994); ATLAS Inner Detector Community, “ATLAS Inner Detector Technical Design Report”, CERN/LHCC/97-16/17, Volumes 1 & 2, (1997); The ATLAS Collaboration, “Calorimeter Performance Technical Design Report”, CERN/LHCC/96-40, (1997); The ATLAS LARG Unit, “Liquid Argon Technical Design Report”, CERN/LHCC/96-41, (1996); The ATLAS/Tile Calorimeter Collaboration, “Tile Calorimeter Technical Design Report”, CERN/LHCC/96-42, (1996); ATLAS Muon Collaboration, “Muon Spectrometer Technical Design Report”, CERN/LHCC/97-22, (1997); ATLAS Magnet Project Collaboration, “ATLAS Central Solenoid Technical Design Report”, CERN/LHCC/97-21; ATLAS Magnet Project Collaboration, “ATLAS Barrel Toroid Technical Design Report”, CERN/LHCC/97-1, (1997); ATLAS Magnet Project Collaboration, “ATLAS End-cap Toroids Technical Design Report”, CERN/LHCC/97-20, (1997); ATLAS Magnet Project Collaboration, “ATLAS Magnet System Technical Design Report”, CERN/LHCC/97-18, (1997).
- [25] G. Corcella *et al.*, *JHEP* **0101**, 010 (2001); hep-ph/0011363; hep-ph/0210213. S. Moretti *et al.*, *JHEP* **0204**, 028 (2002); hep-ph/0204123.

- [26] H. Baer *et al.*, arXiv:hep-ph/0312045v1; H. Baer *et al.*, “Simulating SUSY with ISAJET/ISASUSY 1.0”, “Proceedings of the Workshop on Physics at Current Accelerators and the Supercolliders, Argonne”, ANL-HEP-CP-93-92, C93/06/02 (1993); B. Webber *et al.*, “ISAWIG”, <http://www.hep.phy.cam.ac.uk/~richardn/HERWIG/ISAWIG/>, (2002).
- [27] http://webber.home.cern.ch/webber/hw65_manual.html#htoc62.
- [28] T. Kohno, “LVL2 cosmic muon algorithm documentation”, <https://twiki.cern.ch/twiki/bin/view/Atlas/MuonTriggerDocLvl2Cosmic>, (2007); Private Communication (2007).
- [29] A. Krasznahorkay, Ed. F. Conventi, “LVL1 RPC trigger simulation documentation”, <https://twiki.cern.ch/twiki/bin/view/Atlas/MuonTriggerDocLvl1Rpc>, (2007); N. Kayana, Ed. M. Ishino, “LVL1 TGC trigger simulation documentation”, <https://twiki.cern.ch/twiki/bin/view/Atlas/MuonTriggerDocLvl1Tgc>, (2007).
- [30] M. Boonekamp *et al.*, “Cosmic Ray, Beam-Halo and Beam-Gas Rate Studies for ALTA Commissioning”, ATL-GEN-2004-001 (2004).
- [31] C. Zhang and Y. Ma. Detectability of upgoing sleptons. arXiv:hep-ph/0410353v4.
- [32] S. Hatakeyama *et al.*, Phys. Rev. Lett. **81**, 2016 (1998).
- [33] A. Habig, arXiv:hep-ex/9903041v2.
- [34] T. Toshito, arXiv:hep-ex/0105023v1.
- [35] R. Bailey, “What LHC operation will look like”, Chamonix XIII, pages 219 (2004).
- [36] R. Bailey, “Scheduling LHC operation”, Chamonix XIV, 5 (2005).